RESEARCH ARTICLE

Macromolecular Materials and Engineering
Open Access
www.mame-journal.de

Development and Evaluation of Poly(Lactic-Co-Glycolic Acid) Encapsulated Betulinic Acid Nanocarrier for Improved Anti-Tumor Efficacy

Cyril Tlou Selepe, Khanyisile Sheer Dhlamini, Lesego Tshweu, Lusisizwe Kwezi, Bathabile Ramalapa, and Suprakas Sinha Ray**

Betulinic acid (BA) is a promising natural anti-tumor agent renowned for its activity against various tumor cell types. Despite its favorable profile of low cytotoxicity to normal cells, BA's inherent hydrophobic nature and relatively short systematic half-life impose hurdles for clinical application. This study introduces a strategy to surmount these obstacles by developing a drug delivery system employing poly(lactic-co-glycolic acid) (PLGA)-encapsulated BA nanoparticles (PLGA-BA NPs). Rigorous characterization techniques such as dynamic light scattering (DLS), x-ray diffraction (XRD), and scanning electron microscopy (SEM) analyses are employed to confirm the integrity of the drug within the nanocarriers. The PLGA-BA NPs demonstrated a mean particle size of 196 ± 6.80 nm. XRD analysis demonstrated the amorphous state of the PLGA-BA formulation, a characteristic vital for sustained drug release and enhanced bioavailability. The PLGA-BA NPs exhibited spherical morphology with encapsulation and loading efficiency of 83 ± 9.24% and 7.0 ± 0.4%, respectively, highlighting efficient encapsulation of the drug within the PLGA NPs. In vitro, cytotoxicity assessments demonstrated enhanced anti-proliferative efficacy against breast and lung tumor cells when utilizing PLGA-BA NPs in comparison to free BA. This research underlines the potential of employing the developed PLGA-based nanocarrier to optimize the therapeutic efficacy of BA.

1. Introduction

Cancer, characterized by the uncontrolled proliferation of abnormal cells,[1] remains the prime cause of mortality worldwide. Its high recurrence rate underscores the critical need for specific and effective treatment options. Historically, chemotherapy has stood as the primary first-line approach for the disease, utilizing chemical agents to combat cancer cells, often for patients unresponsive to local excision or radiation therapy.[2] Nevertheless, a notable challenge persists; many chemotherapeutic agents suffer from inherent issues of poor water solubility and adsorption (e.g., doxorubicin), leading to toxic effects on normal cells and limiting the efficacy of cancer therapy.[3,4] Over one-third of the world's best-selling chemotherapeutic drugs are produced from natural products and their derivatives.[5]

Betulinic acid (BA) chemical structure depicted in **Figure 1**, is a naturally occurring pentacyclic triterpenoid extracted from several botanical sources (e.g., birch

C. T. Selepe, K. S. Dhlamini, L. Tshweu, B. Ramalapa, S. S. Ray
Centre for Nanostructures and Advanced Materials
DSI-CSIR Nanotechnology Innovation Centre
Council for Scientific and Industrial Research
Pretoria 0001, South Africa
E-mail: BRamalapa@csir.co.za; rsuprakas@csir.co.za, ssinharay@uj.ac.za

The ORCID identification number(s) for the author(s) of this article can be found under https://doi.org/10.1002/mame.202400283

DOI: 10.1002/mame.202400283

C. T. Selepe, K. S. Dhlamini, S. S. Ray
Department of Chemical Sciences
University of Johannesburg Doornfontein
Johannesburg 2028, South Africa

L. Tshweu, B. Ramalapa
Material Science
Innovation and Modelling (MaSIM)
Faculty of Natural and Agricultural Sciences
North-West University
Mmabatho 2735, South Africa

L. Kwezi
Biomanufacturing Technology Demonstration Group
Council for Scientific and Industrial Research
Pretoria 0001, South Africa

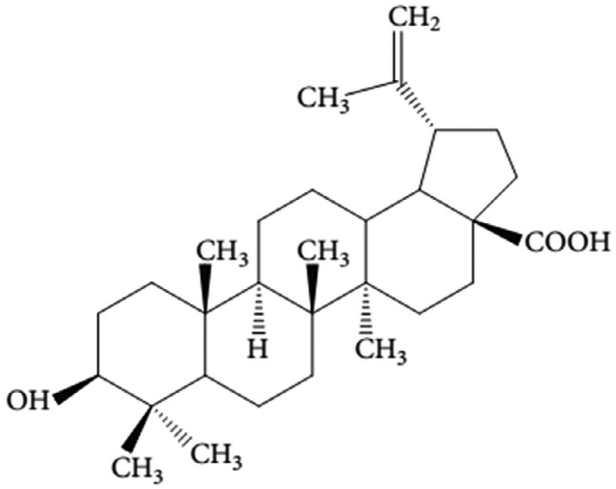

Figure 1. Chemical structure of BA.

tree).[6] This compound boasts a diverse array of pharmacological activities, including anti-malarial, anti-inflammatory, anti-HIV, anti-cancer, anti-depression, and anti-oxidant properties.[7–10] Notably, BA exhibits potent anti-cancer activity against a range of cancer-cell types, including breast, prostate, pancreatic, and colorectal cancer.[11–14] The mechanism underlying BA's anti-cancer effects involves the induction of cancer cell death through mitochondrial membrane permeabilization, resulting in the release of factors such as cytochrome c, Smac, or apoptosis-inducing factor (AIF) in a permeability transition pore-dependent manner. This cascade of events ultimately activates caspases and leads to nuclear fragmentation.[15,16]

Despite its remarkable anti-cancer properties, BA faces several limitations, notably poor water solubility and a short systematic half-life, which diminish its effectiveness and therapeutic potential.[17] Numerous studies have demonstrated that the anti-tumor efficacy of BA can be significantly enhanced when delivered using nanocarriers.[18–20] Therefore, the development of an optimal drug delivery system is imperative to overcome these challenges and maximize factors such as stability, aqueous solubility, controlled drug release, and bioavailability, thereby amplifying its potential as a potent anti-cancer drug.[21]

In recent years, research efforts have been directed toward improving the pharmacokinetic properties of BA using various delivery systems, including liposomes, polymeric nanoparticles (PNPs), and polymeric conjugates, within the realm of nanomedicine.[22–25] NPs are increasing in popularity as drug delivery agents. In particular, polyester-based NPs ensure therapeutic benefits such as tunable release kinetics, versatility, and minimal side effects of the therapeutic agent. Among these polyesters, poly(lactic-co-glycolic acid) (PLGA) has emerged as a promising choice. PLGA has been approved by the Food and Drug Administration (FDA) for clinical use and is known for its excellent properties, such as biodegradability, biocompatibility, stability, and nontoxicity.[26]

It also demonstrates the ability to assemble into nanometric micelles upon interaction with amphiphilic polymers such as polyethylene glycol (PEG), and the capability of entrapping small molecules, such as drug substances, and releasing them sustainably. Notably, the degradation rate of PLGA in the body, the drug encapsulation, and drug release can be finely tuned by altering the ratio of its monomers, lactic acid (LA) and glycolic acid (GA), as well as the molecular weight contributions of each monomer to the polymer.

Despite its favorable qualities, the use of PLGA NPs in drug delivery systems poses several challenges, including poor water stability and rapid clearance from the bloodstream by the liver and spleen, leading to a substantial reduction in drug concentration within tumor tissues. For this reason, extensive research has focused on improving PLGA's ability to protect and efficiently deliver a wide range of drugs to their specific target sites.[27,28] Various protocols have been employed for PLGA NP synthesis, and a wide range of cancer-related drugs have been incorporated in PLGA. Notably, these loaded NPs protect poorly soluble and unstable payloads from the biological environment while being small enough to penetrate capillaries, be internalized, and escape endosomes. For example, a study reported by Pranesh Kumar et al. developed the novel 50:50 PLGA-loaded NPs of BA, tested against free BA for improved treatment of hepatic cancer. The prepared NPs demonstrated a better therapeutic activity against anti-hepatocellular carcinoma (HCC) and were attributed as future candidates for HCC treatment.[29]

Another noteworthy study reported by Dutta et al. focused on the chemical modification of BA by introducing a new functionality at the hydroxyl group of the compound to yield a BA analog. This compound was further encapsulated using a PLGA carrier to improve the colorectal carcinoma treatment. The study revealed that the encapsulated BA analog demonstrated superior anti-tumor activity against loaded BA.[30] Furthermore, Saneja et al. investigated a block copolymer PLGA-PEG to encapsulate BA for improved efficacy against MCF-7 and PANC-1 cells. The study exhibited enhanced cytotoxicity of BA-loaded PLGA-mPEG compared to that of free BA.[31]

Herein, the present study employs a simple single-emulsion approach to develop an effective PLGA-BA NPs formulation. This approach transforms the polymeric system into a nanoscale formulation and enables PLGA NPs to improve the dissolution rate, extend the circulation time, and modulate the biodistribution of BA within the tumors. Due to the inherent limited solubility of PLGA NPs, surfactants were used in the fabrication process to improve their colloidal stability. The addition of surfactants acts by reducing surface tension at the interfaces between different components within the formulation system, resulting in improved solubility, uniform particle size, and better dispersion.[32]

2. Results and Discussion

2.1. Formation and Characterization of PLGA Encapsulated BA Nanoparticles

It has been demonstrated that encapsulating poorly soluble drugs within polymeric NPs improves their pharmacodynamics and therapeutic efficacy, and limits side effects.[33] Here, we have developed a single-emulsion method to produce optimized PLGA-encapsulated BA nanoparticles (PLGA-BA NPs) with the aim of improving the systematic dissolution of BA. The poor solubility of BA in aqueous environments hinders its therapeutic effect and limits its clinical applications.

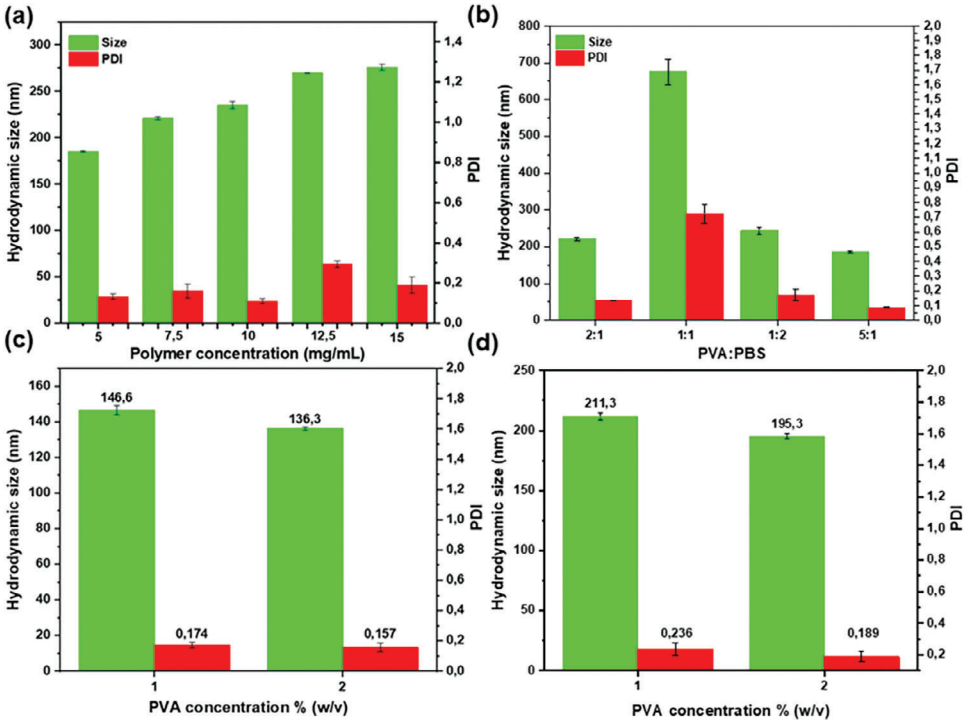

Figure 2. The impact of PLGA concentration on the PS of PLGA-BA NPs obtained via a single emulsion process a), the influence of the aqueous phase (stabilizer: buffer) ratio on the PS b), the effect of the PVA concentration in the aqueous phase: c) PLGA NPs and d) PLGA-BA NPs using 5 mg mL^{-1} of polymer concentration.

The type of organic solvent used to solubilize the drug and polymer in the emulsion process is crucial to controlling the NP size distribution. According to previous studies, the miscibility of organic solvent in water affects the size of the NP.[34,35] Therefore, a water-miscible solvent, acetone was employed in our formulation, resulting in uniform particle size (PS) due to high solvent diffusion, leading to the polymer dispersing more efficiently into water. In addition, we examined the effect of polymer concentration in the organic phase, which is crucial to the formation of NPs. A gradual increase in polymer concentration led to an increase in the size of NPs, as shown in **Figure 2**a. This phenomenon can be explained by the dispersed phase viscosity. The increasing polymer concentration usually yields an increase in the viscosity of the dispersed phase, resulting in larger NP diameters. In addition, the PS is influenced by the nature and concentration of the surfactant, which acts as a stabilizer. Their addition assists in preserving NP suspensions from agglomeration over long storage periods. Experiments were performed with PVA concentrations of 1% and 2% (w/v), keeping other processing parameters the same as demonstrated by Figure 2c,d. The use of 2% PVA was preferred based on the smaller PS of the obtained formulation. Figure 2b illustrates different ratios of the aqueous phase (stabilizer: buffer), a 5:1 ratio was chosen because of the small PS.

FTIR was used to identify the functional groups of BA, PLGA, PLGA NPs, and PLGA-BA NPs. Additionally, the spectra indicated whether there were interactions between the PLGA and BA compound during the encapsulation. **Figure 3** reports the FTIR spectra of various samples. The bands at 2940.9 and 1375 cm^{-1} in the spectrum of BA are attributable to the asymmetric and symmetric C–H stretching vibrations from the methyl and methylene functional groups;[36] while the stretching vibration of C=C is observed at 1641.97 cm^{-1}. The absorption peak at 1683.1 cm^{-1} corresponds to the carbonyl group of BA, i.e., the typical stretching band of C=O vibrations observed in carboxylates. The absorption band observed at 3459.4 cm^{-1} is typical of the well-known O–H stretching vibration.[37] The FTIR spectrum for

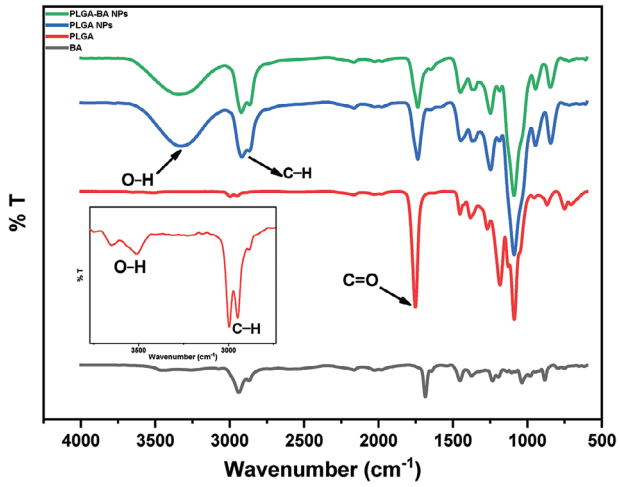

Figure 3. FTIR spectra of BA, PLGA, PLGA NPs, PLGA-BA NPs, and insert of PLGA spectrum zoomed at 2600–3800 cm^{-1}.

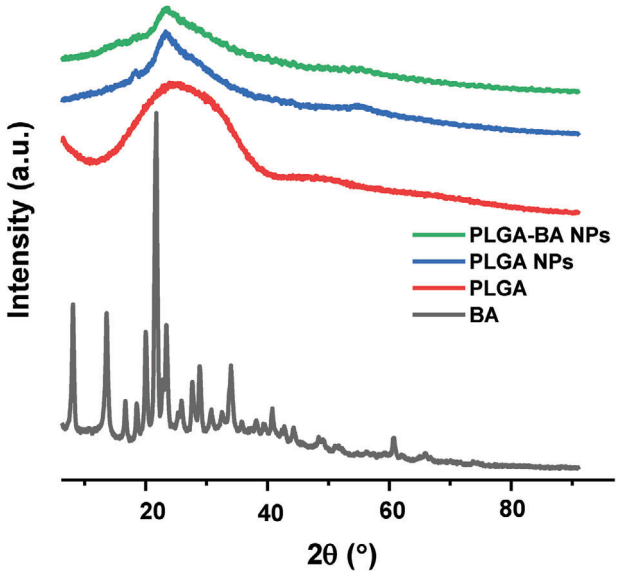

Figure 4. XRD patterns of BA, PLGA, PLGA NPs, and PLGA-BA NPs.

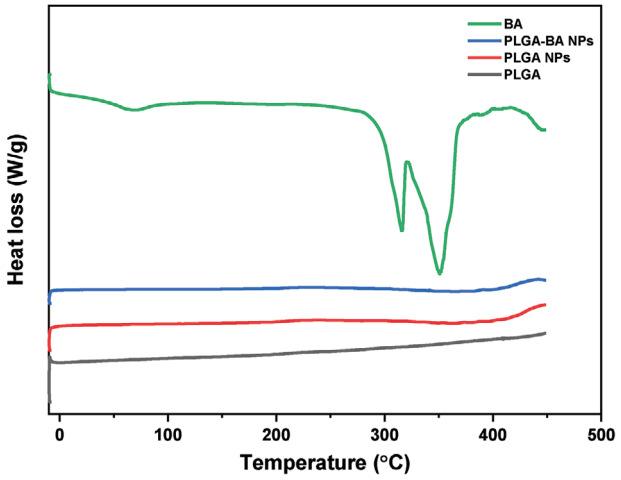

Figure 5. DSC thermograms of PLGA, PLGA NPs, PLGA-BA NPs, and BA.

PLGA NPs showed vibrations that are unique to PLGA, with the strong hydroxyl group absorption seen at a wavenumber of 3329.6 cm^{-1}. The peaks at 1734.5 and 2919.2 cm^{-1} are representative of the C=O and C–H groups, respectively. The FTIR analysis demonstrates no chemical interactions between PLGA and BA molecules in PLGA-encapsulated BA NPs. Also, there are no characteristics of BA peaks observed in the PLGA-BA NPs, indicating efficient encapsulation of BA drug by PLGA matrix.

As shown in **Figure 4**, XRD confirmed the crystalline nature of BA and the amorphous nature of the PLGA-BA formulation. It is an invaluable tool for determining the phase identification of crystalline materials. The XRD pattern of BA shows characteristic diffraction peaks from 8° to 35°, demonstrating that free BA exhibits a high degree of crystallization. Similar results have been observed in another study.[38] Comparatively, the diffraction patterns of PLGA NPs and PLGA-BA NPs showed a wide peak ≈23°. These amorphous characteristics are due to the increased content of lactic acid in comparison to glycolic acid as lactide-rich PLGA copolymers are less hydrophilic, as demonstrated by the XRD pattern of PLGA.[39,40] With increasing LA content in the PLGA copolymer, for example, the LA/GA (75/25) ratio, the overall hydrophobicity of PLGA increases, leading to a lower degradation rate and a gradual drug release rate.[41]

The results indicate that the crystallinity of the BA-loaded formulation is significantly reduced in comparison to that of BA's crystalline form, which aligns with the DSC results, demonstrating the incorporation of BA into the amorphous PLGA formulation. This result of the amorphous nature of PLGA-BA NPs is similar to what is reported in the literature.[42] Moreover, the diffraction pattern of PLGA-BA NPs closely resembles that of PLGA NPs, suggesting that the encapsulation process did not alter the polymeric structure of the PLGA, and the BA drug molecules were successfully encapsulated by PLGA.

According to the literature, an amorphous formulation can be substantially more soluble than the corresponding crystalline formulation.[43] This increase in solubility can lead to bioavailability benefits. It is also important to note that the biodegradation rate of amorphous material is higher because of the less oriented structure. The amorphous forms of drug formulations form intermolecular hydrogen bonds with water more easily than the crystallized forms. The crystalline form is more rigid and has stronger intramolecular forces, which makes it less likely to form hydrogen bonds and results in a lower dissolution rate.[44] Therefore, the overall results demonstrated that the encapsulation process used was adequate to obtain a fine lyophilized amorphous formulation, which is necessary for an effective dissolution rate.

DSC was used to examine the changes in the crystal forms of the drug in the preparations and their interactions. An analysis of the thermal properties of BA, PLGA, PLGA NPs, and PLGA-BA NPs was conducted, and DSC thermograms of various samples are reported in **Figure 5**. The thermogram of the free BA demonstrated two sharp endothermic peaks at 316.23 and 351.23 °C.[45,46] The presence of these sharp and well-defined melting endothermic peaks in the DSC thermogram indicates a crystalline nature of BA. The first heating scan is crucial for identifying the melting temperature (T_m) of a crystalline drug. This is the temperature at which the BA drug transitions from a solid-crystalline state to a liquid state. It provides valuable information about the thermal stability of the drug and is a key parameter in understanding its processing and formulation characteristics. On the contrary, this peak completely disappeared in the thermal profile of the PLGA-BA NPs formulation, suggesting no crystallinity in the PLGA-BA NPs. This suggests that the crystal structure of the BA is minimized in the PLGA-BA NPs and exists in an amorphous structure of the formulation.[47] Furthermore, no melting points were observed for PLGA, PLGA NPs, and PLGA-BA NPs, which confirmed their amorphic nature. There was no presence of a sharp endothermic peak of BA (T_m) in the PLGA-BA NP compared to free BA (≈300 °C) indicating that there was no interaction between the two components in the PLGA-BA NPs. The appearance of the same thermograms between the PLGA NPs and PLGA-BA NPs is attributed to the amorphous nature of the pure PLGA copolymer. These results demonstrate reduced crystallinity of the BA compound during the preparation of the formulation, as supported by the XRD results.

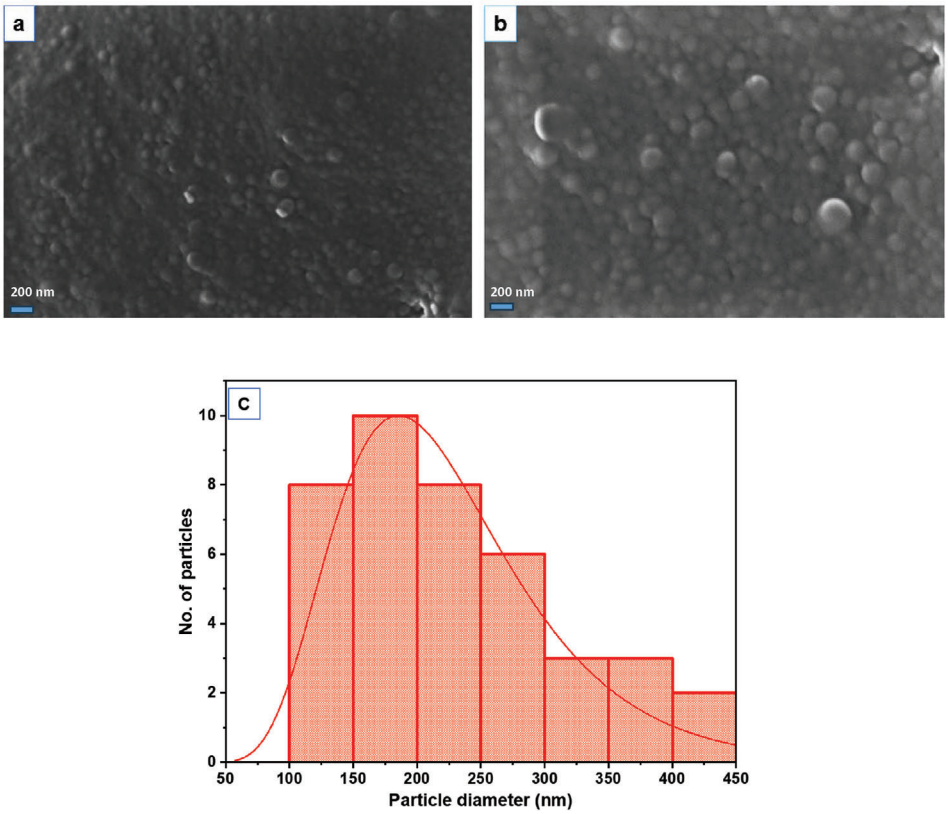

Figure 6. SEM micrograph of a) PLGA NPs, b) PLGA-BA NPs, and c) particle size distribution of PLGA-BA NPs.

The SEM micrograph of the PLGA NPs and PLGA-BA NPs (**Figure 6**a,b) reveals that the formulations exhibited a smooth spherical shape in morphology; these spherical particles exhibit distinct sizes and uniform particles that are widely distributed. Figure 6b demonstrates that the spherical morphology did not change after the encapsulation of BA, indicating a successful encapsulation process. As the PLGA-BA NPs were crafted using the emulsion method, the formulation exhibited a somewhat dispersed physical state of the spherical nanostructures. NPs are prone to aggregation due to potent van der Waals forces, often forming small clusters.[48] The mean PS determined by ImageJ is (225592 ± 85392) nm, which agrees with the results obtained by the DLS technique. In addition, the slight increase in PS size is not significant. The PS distribution in Figure 6c indicates that most particles are in the 150–200 nm region. The SEM images of NPs show a slightly larger size than the DLS measurements (**Table 1**). This might be due to the nature of the samples used for SEM and DLS measurements.[49]

Table 1. Physical-chemical properties of developed formulation (n = 3, mean ± SD).

Formulation	Mean PS [nm]	PDI	ZP [mV]
PLGA NPs	166.9 ± 0.961	0.112 ± 0.019	−3.64 ± 0.732
PLGA-BA NPs	215.7 ± 9.790	0.333 ± 0.021	−6.03 ± 0.429
PLGA-BA NPs FD	196 ± 6.80	0.235 ± 0.034	−9.25 ± 0.133

FD, Freeze-dried; PS, particle size; PDI, poly dispersity index; ZP, zeta potential.

The results obtained from the DLS analysis are presented in Table 1. The mean PS of the NPs ranged from 166.9 to 215.7 nm, whereas the mean Zeta potential (ZP) ranged from −3.64 to −9.25 mV. The negative surface charge of the NP formulations is due to the characteristic nature of acidic PLGA. It is widely recognized that two crucial parameters, PS and ZP, play a pivotal role in evaluating the stability of nanosystems and provide insight into the physiochemical properties of the formulation, including dissolution rate, saturation solubility, and physical stability. ZP serves as an indicator of the ability of NPs to remain stably dispersed in suspension.[50] The freeze-dried PLGA-BA NPs formulation exhibited a PS of 196 ± 6.80 nm and a ZP of (−9.25 ± 0.133) mV, demonstrating a well-distributed system supported by a low PDI of 0.235 ± 0.034. The decrease in PS after freeze-drying can be attributed to a combination of physical stresses during freezing and sublimation, structural breakdown due to shear forces, changes in pressure, and particle disaggregation.[51] Based on statistical analysis, the formulation had no significant difference in PS before and after freeze-drying. There is also no significant change in the PDI values before and after freeze-drying, indicating a homogenous particle distribution with uniform sizes. Therefore, this PS is an ideal range for NPs to promote tumor accumulation. Additionally, particle sizes greater than 300 nm are reported to easily be removed from the bloodstream due to recognition of the reticuloendothelial system (RES).[52,53] The graphic representation of PLGA-BA NPs in **Figure 7**a,b further corroborated the uniform distribution of PLGA-BA NPs, confirming the robust physical stability of the formulation.

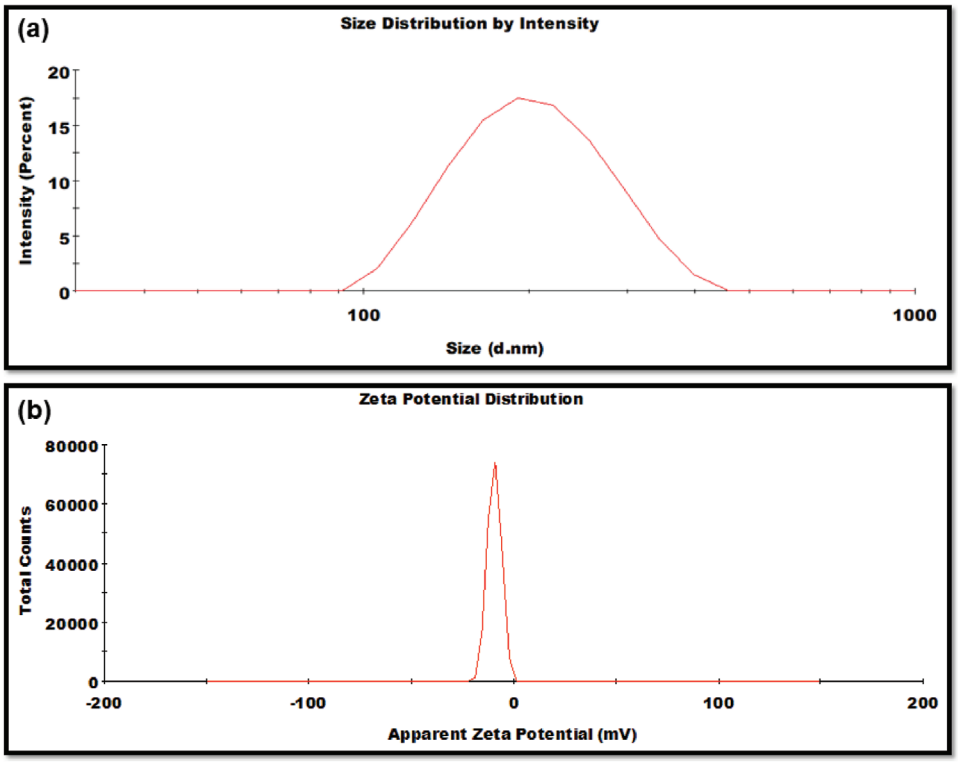

Figure 7. Graphs representing a) PS and b) ZP of PLGA-BA NPs.

Figure 8 shows the digital photograph of PLGA-BA NPs and BA dissolved in water. The PLGA-BA nano-formulation showed clear opalescence in Figure 8a, which confirms the uniform distribution of PLGA-BA NPs to enhance the physical stability of the formulation. This opalescence results from dispersed particles, such as BA particles, PLGA NPs, or other colloidal components. Therefore, a well-dispersed system with finely homogenous particles contributes to stability by preventing particle aggregation. It is commonly associated with emulsions. In stable (O/W) emulsions, the dispersed phase (e.g., oil droplets) is uniformly distributed and does not coalesce or separate from the continuous phase. Furthermore, the opalescent appearance of this formulation suggests that the emulsifying agents effectively stabilize the system. However, the BA compound in Figure 8b is shown to not dissolve in water, as reported in the literature.[54] It is apparent that hydrophobic BA precipitates in water as a result of its poor affinity for water molecules, leading to low solubility. This compound is composed of molecules that do not interact favorably with water molecules. This lack of interaction leads to the drug molecules aggregating together rather than dispersing in water, causing precipitation. Conversely, when encapsulated, the hydrophobic BA is surrounded by materials that can interact with water more favorably, allowing the drug to be dispersed or dissolved. The formulation forms a protective hydrophilic shell around BA. This shell interacts with water, effectively increasing the solubility of the encapsulated BA, confirming that the formulation improves the dissolution rate.

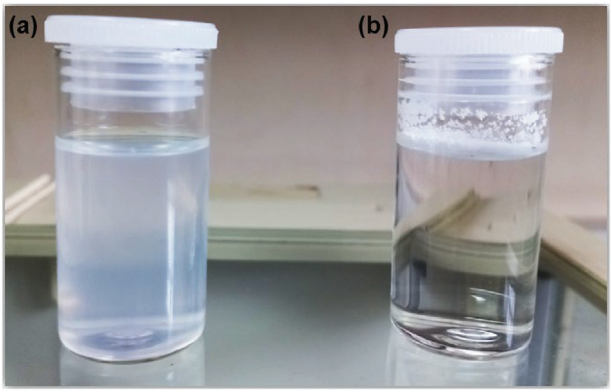

Figure 8. The appearance of a) PLGA-BA NPs and b) BA dissolved in water.

Prior research findings[55] established that the solubility of BA in water stands at 0.02 μg mL^{-1}. In the current study, the HPLC chromatogram depicted in **Figure 9** demonstrates the water solubility of PLGA-BA NPs surpasses that of free BA. Furthermore, Figures S1–3 show various HPLC chromatograms of the BA standard samples, with correlating retention times. In addition, various formulations are also presented, indicating that the retention time correlates to that of the standard samples despite the method used to solubilize the formulations. The data in Figure 9 suggested that the dissolution rate of PLGA-BA NPs (48.88 μg mL^{-1}) was higher than that of BA. These results validate that the incorporation of stabilizers with BA to create the PLGA-BA nano-formulation has the potential to markedly elevate the dissolution rate of BA. The reduction in NP size substantially increases the surface area available for interaction with the solvent, and the effective stabilizers ensure an even distribution of drug

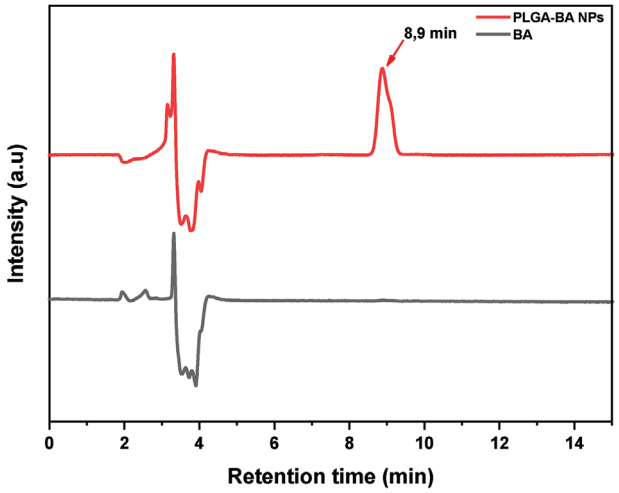

Figure 9. HPLC chromatogram of BA and PLGA-BA NPs post 24 h incubation time.

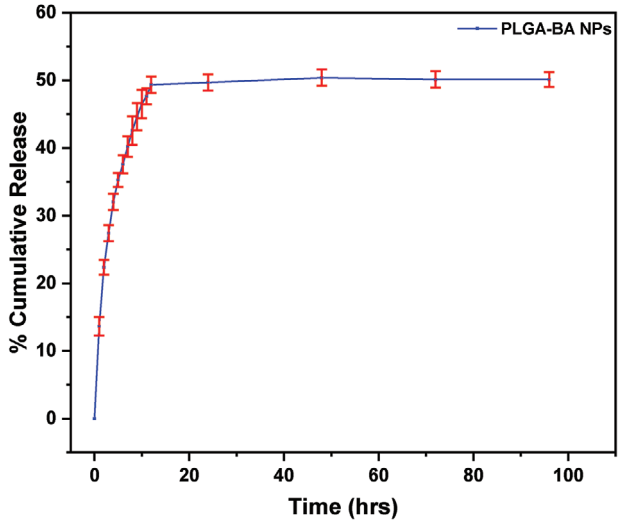

Figure 10. Release profile of BA from PLGA-BA nanocarrier into PBS solution at pH 7.4 within 96 h.

Table 2. The stability results of PLGA-BA NPs ($n = 3$, mean ± SD).

Storage Time [Days]	PS [nm]	PDI	ZP [mV]
0	196 ± 6.80	0.235 ± 0.034	−9.25 ± 0.13
30	195.2 ± 6.26	0.256 ± 0.020	−14.5 ± 5.09

PS, particle size; PDI, polydispersity index; ZP, zeta potential.

particles within distilled water, thereby hindering particle aggregation and enhancing BA stability. Consequently, nanoscale technology emerges as an efficient approach for augmenting the BA dissolution rate, particularly in cases where this rate represents a critical determinant in systemic absorption processes.

As shown in **Table 2**, there was no change in PS over a 30-day storage period as well as no variation in PDI values. It was determined that the PS and PDI remained uniform in appearance and had no significant changes during storage.

The quantification of BA within PLGA was assessed using HPLC. Following centrifugation to separate the components, the supernatant was collected and subsequently analyzed at 210 nm, a wavelength known for its characteristic absorption of BA. After comparing the concentration of the BA remaining in the supernatant with that of the initial BA solution, the loading of BA and the encapsulation efficiency were calculated as presented in **Table 3**. The high encapsulation efficiency demonstrates that the BA is efficiently encapsulated into the PLGA carrier system without significant loss or leakage. This results in a more effective drug delivery system. High encapsulation efficiency is usually achieved with hydrophobic drugs when solvent evaporation is used in the preparation of NPs. Low water solubility prevents material from entering the external phase. This applies to BA, a hydrophobic compound with low aqueous solubility.[56,57] However, other factors should also be considered. While high encapsulation efficiency is a positive indicator, the overall success of the formulation methodology must also be assessed based on other parameters, such as stability, biocompatibility, release kinetics, and therapeutic effect.

Table 3. Drug loading and encapsulation efficiency of the formulation ($n = 3$, mean ± SD).

Formulation	DL [%]	EE [%]
PLGA-BA NPs	7.0 ± 0.4	82.88 ± 9.24

DL, drug loading; EE, encapsulation efficiency.

2.2. In Vitro Release Studies

To investigate the impact of BA formulations on the release kinetics, in vitro release of BA loaded in PLGA NPs was performed at physiological temperatures (37 °C) using PBS (pH 7.4), and the release studies were evaluated in triplicates, as shown in **Figure 10**. The PLGA-BA nano-formulation exhibited a seemingly biphasic release pattern consisting of a burst release (<12 h), followed by a possible continuous period of minimal to negligible drug release due to the final loss of drug in the PLGA matrix. The burst release pattern can help suppress the tumor growth in a short period, whereas the potential sustained release could offer the possibility of a continuous battle against tumor cells.[58]

There are usually two ways to explain this burst release pattern of PLGA-BA NPs. The initial burst of drug release is related to the type of drug, the concentration of the drug, and the hydrophobicity of the polymer. The rapid release of therapeutic molecules may occur due to the heterogeneous distribution of the drug distribution; for instance, therapeutic molecules embedded in or loosely associated with the surface layer. In addition, random scission of PLGA significantly decreases the molecular weight of the polymer. However, this phase does not allow significant weight loss and does not form a soluble monomer product.[59,60]

Furthermore, the release of drug molecules through the pores and cracks is associated with variation in particle morphology. The water within the matrix hydrolyzes the polymers into oligomers and soluble monomers. This creates a gap where the drug is released through diffusion and erosion until polymer sol-

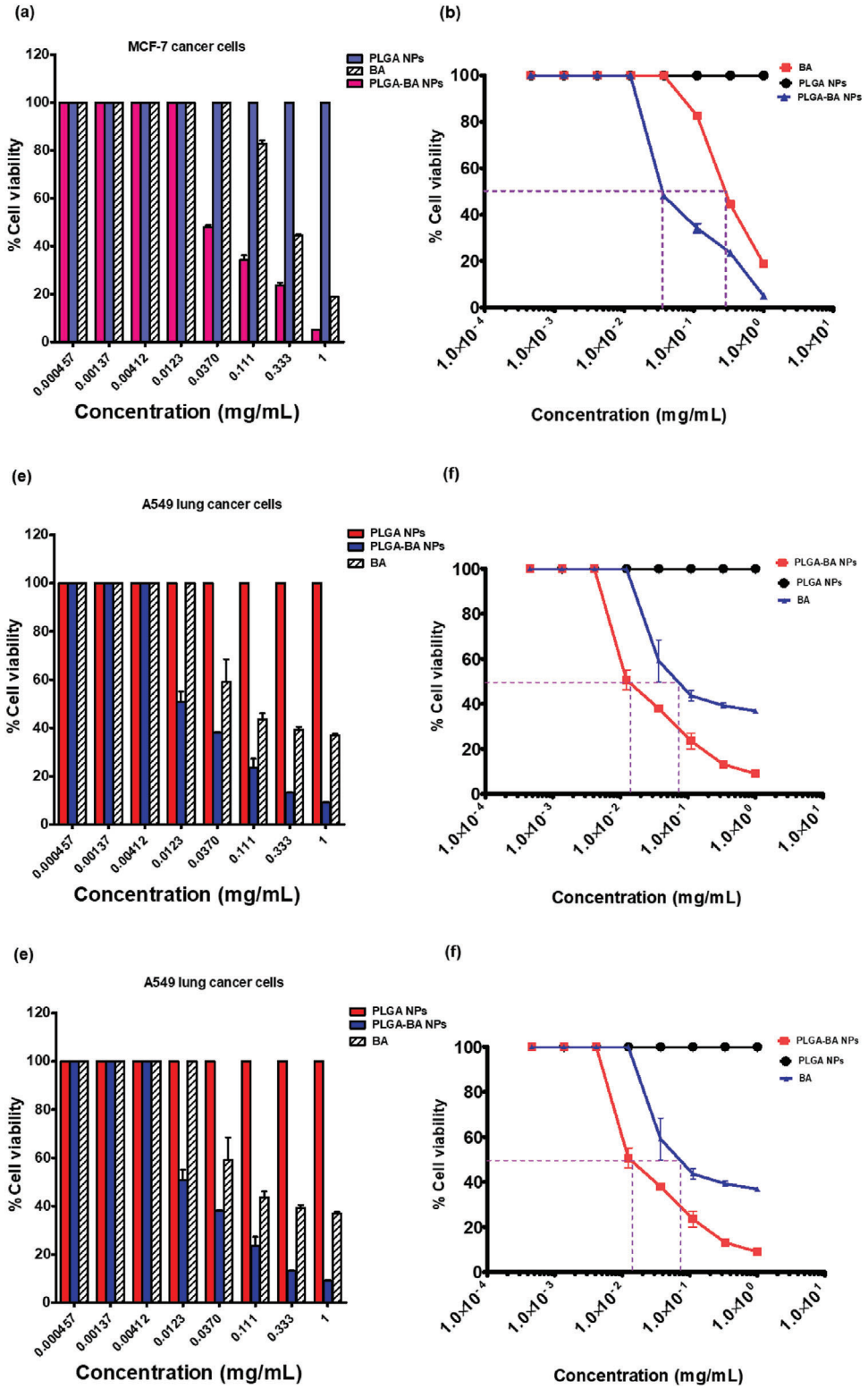

Figure 11. a) Cell viability of, b) MCF-7 breast cancer cells; c,d) Caco-2 colon cancer cells; and e,f) A549 lung cancer cells treated with BA, PLGA NPs, and PLGA-BA NPs for 72 h.

ubility is complete.[61] Since only 50% of the BA is released until 96 h at pH 7.4, this delivery system could help maintain and retain controlled drug release for a more extended period before excretion, thus favoring enhanced bioavailability and stability.

2.3. Cytotoxicity Studies

Plant-derived triterpenoid compounds have attracted considerable interest due to their numerous health benefits, including their antioxidative, anti-inflammatory, and anti-tumor properties. These properties strongly depend on their bioavailability in the organism.[62] BA specifically, has been studied for its anti-tumor properties. However, its medical applications are limited by its high hydrophobicity, which is associated with low bioavailability. In this study, PLGA-BA NPs were synthesized using a simple, scalable emulsion technique, with the aim of developing a BA formulation with increased solubility and enhanced bioavailability. Cytotoxicity studies were conducted to evaluate the effect of encapsulation on the anti-tumor activity of BA. The investigations were conducted against the MCF-7 breast cancer cell line, the Caco-2 colon carcinoma cell line, and the A549 tumorigenic lung cell line.

The cytotoxicity effect of BA, PLGA NPs, and PLGA-BA NPs at different concentrations on MCF-7, Caco-2, and A549 cell lines was examined employing the MTT assay. This assay is based on the theory that an increase or decrease in viable cells is linearly related to mitochondrial activity, which is reflected by the exchange of tetrazolium salt into dissolved formazan crystals.[63] The safety of PLGA has widely been documented because of its remarkable properties, but the reformulated PLGA NPs may be cytotoxic and have, therefore, been evaluated. As shown in **Figure 11**a,b, the results demonstrated that PLGA-BA NPs inhibited MCF-7 cell growth in a dose-dependent manner. In addition, a significant decrease in living cells was found when cells were exposed to concentrations from 1 to 0.0123 mg mL^{-1} of sample solutions.

Figure 11c,d exhibited that the cytotoxicity was also based on dose correlation when PLGA-BA NPs were exposed to Caco-2 cells. Simultaneously, the exposure of the PLGA NPs to both cancer cell lines revealed no significant toxicity, implying the excipients' inhibitory effect on cells was negligible. It has already been reported that biodegradable PLGA is safe for different types of cells, the safety depends on the concentration of NPs and exposure time.[64] Xiong et al. studied the cytotoxicity of PLGA NPs on normal cells, focusing on the metabolic activity of macrophages.[65] The results of our study indicated that the toxic concentration 50 (TC_{50}) values of PLGA-BA NPs on MCF-7 tumor cells were lower than BA after the same incubation time and TC_{50} values of PLGA-BA NPs on Caco-2 tumor cells were slightly greater than that of BA (as shown in **Table 4**). This parameter describes the concentration of a substance at which 50% of cells were affected or killed. It is often used in dose-response studies to assess the cytotoxic or inhibitory effects of a drug or compound on cancer cells. It is also evident that PLGA-BA NPs have superior cytotoxicity on MCF-7 than in Caco-2 cells.

Table 4. Depicts the TC_{50} (mg mL^{-1}) of the samples on different cell lines.

Sample	MCF-7	Caco-2	A549
BA	0.287	0.0447	0.0750
PLGA-BA NPs	0.0355	0.0926	0.0139

Figure 11e,f exhibits the cytotoxicity based on a dose-dependent manner when PLGA-BA NPs were exposed to A549 cells. Simultaneously, the results of the drug-free NPs on lung cancer cells revealed that no significant toxicity was found, implying that the inhibitory effect of the excipients on cells was negligible. These results also indicate that the TC_{50} value of PLGA-BA NPs is lower than BA on MCF-7 and A549 cells, which is consistent with the results of other cell lines after the same incubation period. In summary, PLGA-BA NPs have superior cytotoxicity on MCF-7, and A549 cells compared to BA. PLGA-BA NPs demonstrate reduced cell proliferation and cell viability of the tumor cells compared to BA due to the enhanced solubility of the PLGA-BA nano-formulations. A previous study reported the increased solubility of BA achieved through polymeric conjugation, which results in improved cytotoxicity and induction of apoptosis in pancreatic cancer cells.[66]

It is well documented that NPs can deliver normally insoluble drugs to tumor sites at higher concentrations. Previous studies have shown that drug-loaded NPs can enter tumor cells through endocytosis and release drugs.[67,68] This approach could avoid the P-glycoprotein efflux, thereby overcoming the resistance mechanisms of tumor cells. The chemoresistance exhibited by cancer cells is one of the reasons why traditional therapy is less effective in combating cancer.[68] Meanwhile, cell viability increased significantly with decreasing sample concentration, indicating that the therapeutic effect of BA in the PLGA-BA NPs is concentration-dependent. In vitro cytotoxicity studies of encapsulated BA versus native drugs that demonstrated improved efficacy against HT-29 cells and HCC were reported by Kumar et al.[29] and Dutta et al.,[30] respectively. Hence, additional evidence on the antitumor properties of BA against multiple tumor cells is provided. Overall, the results demonstrated that the PLGA-BA NPs had enhanced cytotoxicity compared to native BA, possibly due to the effective endocytosis of the PLGA-BA NPs in the cells. The results obtained were also in line with earlier reports in which bioactive molecules encapsulated in PLGA showed superior cytotoxicity compared to native molecules.[69–71]

3. Conclusion

Our pursuit of enhancing the solubility, bioavailability, and shelf-life of the plant-derived BA led to the development of an optimized PLGA-BA nanocarrier that is simple to produce and easily scalable. The advanced polymeric drug delivery system was produced via an ease-of-use emulsification evaporation method. The remarkably diminutive particle size and uniform morphology of PLGA-BA NPs underscores their proficiency in reducing the size of BA particles while ensuring consistent and even distribution. A series of rigorous characterization techniques, including FTIR, XRD, and DSC analyses, have confirmed that the drug remains unaffected by excipients and experimental manipulations. Notably, PLGA-BA NPs have exhibited markedly heightened cytotoxicity against MCF-7, and A549 cell lines compared to free BA. It is imperative to highlight that while these findings hold immense promise, the distribution of PLGA-BA nano-formulation within the human body and the precise mechanisms underlying

its efficacy in inhibiting tumor cell growth warrant further comprehensive investigation. These endeavors lay the pivotal theoretical groundwork for future advancements and refinements in this critical field of study.

4. Experimental Section

Materials: Resomer RG 753 H Poly(D, L-lactide-co-glycolide) — PLGA (75:25), Mw 54–69 kDa was obtained from Evonik, polyvinyl alcohol (PVA) 87–89%, sodium chloride (NaCl) ≥ 99.0%, potassium chloride (KCl) ≥ 99.0%, sodium phosphate dibasic (Na_2HPO) ≥ 99.0%, potassium phosphate monobasic (KH_2PO_4) ≥ 99.0%, phosphate buffer saline (PBS), Acetone (C_3H_6O) ≥ 99.5%, and TWEEN 80 were purchased from Sigma–Aldrich and BA was supplied by DB Fine Chemicals specialties. Deionized water was used to prepare the solutions. All the reagents are of analytical grade and were used as received.

Preparation of PLGA-BA NPs: PLGA-BA NPs were developed by employing the single emulsion solvent evaporation method. Briefly, a calculated amount of PLGA (20 mg) and BA (10 mg) were co-dissolved in acetone, and 50 µL of TWEEN 80 was added to the mixture. The continuous phase was produced by the mixture of 2% (w/v) PVA in a solution of PBS buffer (pH 7.4). The organic phase containing the PLGA, surfactant, and BA was added to the continuously stirring aqueous solution at a dropwise interval to produce a stable oil in water (O/W) emulsion. The acetone was evaporated under magnetic stirring at 430g and 25 °C at low extraction. The developed NPs were acquired via centrifugation at 14,200g for 20 min at 4 °C (Allegra 64R centrifuge, BECKMAN COULTER) and further washed with deionized water through centrifugation to eliminate excess PVA and unencapsulated drug. This was followed by freezing at −80 °C and then lyophilization was performed on a Telstar LyoAlfra10 freezer dryer (Spain) at −60 °C with 0.3 mBar to obtain the powder form. The same procedure was used to synthesize PLGA NPs without BA.

Physicochemical Characterization: The particle size, polydispersity index (PDI), and zeta potential of PLGA NPs and PLGA-BA NPs were measured using the ZETASIZER Nano series (MALVERN INSTRUMENTS, Worcestershire, UK). The measurements were performed on diluted samples at 25 °C and each sample was measured in triplicate. All data were represented as the mean ± standard deviation (SD). Attenuated Total Internal Reflectance-Fourier transform infrared spectroscopy, ATR-FTIR (PerkinElmer, Inc., Shelton, CT, USA) measurements were conducted over the wavenumber range of 500–4000 cm^{-1} with 4 cm^{-1} resolution, and 32 scans were recorded for each experiment. Approximately 2 mg of each sample was placed on the FTIR plate for measurements, and all spectra were recorded against the background of the air spectrum. X-ray diffraction, XRD (X'Pert PRO Malvern PANalytical, UK) patterns of the BA, PLGA, PLGA NPs, and PLGA-BA NPs were obtained using Cu Kα radiation (λ = 0.15405 nm) to produce measurements in the 2θ range from 5° to 90° at 45 kV and 40 mA operational conditions. The powder samples were spread evenly on an XRD sample holder, flattening the surface to ensure consistent diffraction. For bulk solid (foam-like samples), adhesive was used to hold the sample in place to ensure the sample had a flat surface for XRD analysis. The samples were analyzed using a scanning electron microscope (SEM, JSM7500F, JEOL, Japan) with an accelerating voltage of 20 kV to observe the surface morphology of the PLGA NPs and PLGA-BA NPs. The NPs were affixed onto carbon stubs using double-sided carbon adhesive tape. Subsequently, a conductive carbon coating was applied to the sample using a high-vacuum evaporator under an argon atmosphere. Differential scanning calorimetry (DSC, model Q2000, TA Instruments, USA) was used to measure the thermal properties of PLGA, BA, PLGA NPs, and PLGA-BA NPs. The dried samples in the range of 5–6 mg were loaded and sealed into an aluminum pan and scanned between −10 and 450 °C at a rate of 10 °C min^{-1} under a constant purging nitrogen atmosphere.

Drug Loading Capacity and Encapsulation Efficiency: To determine the drug loading capacity of the PLGA-BA NPs, a methanolic stock solution of BA was prepared and analyzed using high-performance liquid chromatography (HPLC) (Shimadzu Nexera, Japan), the objective of the analysis was to determine the total amount of drug encapsulated within the polymeric nanocarrier. A calibration curve was generated through successive dilutions of the stock solution. HPLC analysis was performed using a C18 column (Lichrosphere RP-18, 250 mm × 4 mm × 5 µm) operated at 30 °C with a UV detector set at 210 nm. The mobile phase consisted of acetonitrile and methanol (80: 20% v / v) with a flow rate of 0.5 mL min^{-1}. To quantify the encapsulation capacity, the PLGA-BA NP samples were dispersed in a mixture of water and methanol (1:1) to generate sample solutions. The samples were centrifuged for 30 min at 4 °C and 14 200 g, separating the supernatant and determining the absorbance. The drug loading capacity (%DL) and encapsulation efficiency (%EE) were calculated using the following formulae:

$$\%DL = \frac{mass\ of\ BA\ within\ the\ NPs}{mass\ of\ NPs} \times 100\% \quad (1)$$

$$\%EE = \frac{mass\ of\ BA\ loaded\ within\ the\ NPs}{mass\ of\ BA\ in\ the\ initial\ formulation} \times 100\% \quad (2)$$

In Vitro Release Study: In vitro release of the BA from PLGA-BA NPs was examined in PBS solution at a physiological pH of 7.4. The objective of the study was to determine the amount of drug released at specific time points; thus, it was crucial to achieve total dissolution for accurate measurement of the amount of drug released. The samples were incubated at 37 °C in PBS buffer (1 mg mL^{-1}) and aliquots were removed at different time points. The aliquots were centrifuged at a higher centrifugation speed of 21 400 g for 15 min at 4 °C, to separate NP debris from the drug solution and prevent interference with the drug analysis. The supernatant-containing drug was diluted using a methanolic solution to ensure the dissolution of the drug before HPLC analysis.

Solubility Study: The objective of the study was to demonstrate and compare the solubility and dissolution of similar concentrations of pure BA and PLGA-encapsulated BA, in water.

Briefly, the pure BA and PLGA-BA NPs were dissolved in deionized water at a total BA concentration of 1 mg mL^{-1}. Afterward, the solution was incubated with a gentle shaking at 85 g in a constant temperature shaker at 37 °C for 24 h. The suspension was centrifuged at 14 200 g for 20 min at 4 °C and filtered using a 0.22 µm micropore film to separate the NP debris from the micronized BA. The supernatant was analyzed using HPLC at a maximum of 210 nm.

Stability Studies: The formulation stability of PLGA-BA NPs was evaluated after storage for 30 days at 4 °C. Approximately 0.5 mL of the nanoformulation was dispersed in 2 mL of distilled water and vortexed for 2 min to produce a clear solution. In terms of freeze-dried samples, ≈1 mg of each sample was weighed and reconstituted in 2 mL of deionized water, followed by vortexing. Dynamic light scattering (DLS, Malvern PANalytical) measurements were taken on days 0 and 30.

In Vitro Cytotoxicity Assays—Cell Culture Growth and Treatment Conditions: MCF-7, Caco-2, and A549 cancer cell lines were employed to study the cytotoxicity and anti-cancer effects of BA and PLGA-BA NPs. These cells were grown in a 75 cm^2 culture container (Thermo. Fisher Inc.) and maintained in Dulbecco's modified Eagle medium (DMEM), supplemented with 200 U mL^{-1} penicillin, 270µg mL^{-1} streptomycin and 10% (v/v) of fetal bovine serum (FBS). The cells were incubated at 37 °C/5% CO_2, and after reaching 80% confluence, cells were passaged three times before the cytotoxic assays were initiated.

In Vitro Cytotoxicity Assays—Cytotoxicity Evaluation: The cytotoxicity assays for the samples were performed by first seeding the MCF-7, Caco-2, and A549 cells in a 96-well plate for 24 h at 37 °C and 5% CO_2. Following the 24-h incubation, a 3-fold serial dilution was performed with free BA in 0,1% DMSO, free NPs, and reformulated BA in PBS, starting with a concentration of 1 mg mL^{-1}. To the plate containing cells, 100 µL of the sample serial dilutions were added except in the cell control wells. Following 72 h of incubation, the media was removed and replaced with 25 µL of 3-(4,5-Dimethylthiazol-2-yl)-2,5-diphenyltetrazolium bromide (MTT) reagent (5 mg mL^{-1}) (Sigma–Aldrich, St. Louis, MO). Subsequently, the formazan product was allowed to form from viable cells for 3 h of incubation at 37 °C.

The MTT reagent was removed after incubation, and 100 µL DMSO was added and then incubated for 15 min at 25 °C. Afterward, the Microplate was read at a wavelength of 620 nm using the Tecan Infinite F500 luminometer, and the experiments were conducted in triplicates. The survival rate of cells (% Cell viability) was measured using the equation below:[72]

$$\%\ \text{Cell viability} = \frac{Absorbance_{sample}}{Absorbance_{control}} \times 100\% \quad (3)$$

In Vitro Cytotoxicity Assays—Statistical Analysis: The experiments were performed in triplicates, and each data point represents the mean and standard deviations. The TC_{50} values were obtained from an analysis of GraphPad Prism 5 software (GraphPad Prism software, San Diego, CA, USA). A one-way ANOVA analysis was used to determine the statistical significance. A p-value of < 0.05 was considered statistically significant.

Supporting Information

Supporting Information is available from the Wiley Online Library or from the author.

Acknowledgements

The authors acknowledge financial support from the Department of Science and Innovation (Grant number C6A0056).

Conflict of Interest

The authors declare no conflict of interest.

Author Contributions

C. T. S. performed the conceptualization, investigation, methodology, and data curation of the study, taking primary responsibility for the original draft preparation, review, editing, and visualization of findings. K. S. D. and L. T. provided validation of the research and wrote, reviewed, and edited the manuscript. L. T. performed validation and wrote, reviewed and edited the manuscript. L. K. performed conceptualization, supervision, and manuscript review and editing. S. S. R. performed conceptualization, securing resources, supervision, project administration, and funding acquisition, along with contributing to manuscript review and editing. B. R. performed conceptualization, methodology, and formal analysis, providing essential resources and original draft preparation, project administration, and wrote reviewed and edited the final manuscript.

Data Availability Statement

The data that support the findings of this study are available from the corresponding author upon reasonable request.

Keywords

anti-tumor, betulinic acid, drug delivery, nanocarrier, poly (lactic-co-glycolic acid)

Received: August 2, 2024
Revised: October 29, 2024
Published online:

[1] A. G. Waks, E. P. Winer, *J. Am. Med. Assoc.* **2019**, *321*, 288.
[2] H. Zhang, H. Xu, C. R. Ashby Jr, Y. G. Assaraf, Z. S. Chen, H. M. Liu, *Med. Res. Rev.* **2021**, *41*, 525.
[3] S. Md, N. A. Alhakamy, P. Sharma, M. S. Ansari, B. Gorain, *J. Drug Target.* **2022**, *30*, 801.
[4] S. Bamrungsap, Z. Zhao, T. Chen, L. Wang, C. Li, T. Fu, W. Tan, *Nanomedicine* **2012**, *7*, 1253.
[5] R. Watkins, L. Wu, C. Zhang, R. M. Davis, B. Xu, *Int. J. Nanomed.* **2015**, *10*, 6055.
[6] H. Lou, H. Li, S. Zhang, H. Lu, Q. Chen, *Molecules* **2021**, *26*, 5583.
[7] K. D. Kim, H. Y. Jung, H. Ryu, B. Kim, J. Jeon, H. Yoo, C. Park, B. H. Choi, C. K. Hyun, K. T. Kim, *Nutr. Metab. Cardiovasc. Dis.* **2019**, *29*, 409.
[8] A. Hordyjewska, A. Ostapiuk, A. Horecka, J. Kurzepa, *Phytochem. Rev.* **2019**, *18*, 929.
[9] P. Yogeeswari, D. Sriram, *Curr. Med. Chem.* **2005**, *12*, 657.
[10] R. Mukherjee, V. Kumar, S. K. Srivastava, S. K. Agarwal, A. C. Burman, *Anti-Cancer Agents Med. Chem.* **2006**, *6*, 271.
[11] R. Tiwari, A. Puthli, S. Balakrishnan, B. Sapra, K. Mishra, *Cancer Investig.* **2014**, *32*, 402.
[12] J. Shin, H. J. Lee, D. B. Jung, J. H. Jung, H. J. Lee, E. O. Lee, S. G. Lee, B. S. Shim, S. H. Choi, S. G. Ko, *PLoS One* **2011**, *6*, e21492.
[13] Y. Guo, H. Zhu, M. Weng, C. Wang, L. Sun, *BMC Complement. Med. Ther.* **2020**, *20*, 1.
[14] A. Zeng, H. Hua, L. Liu, J. Zhao, *Bioorg. Med. Chem.* **2019**, *27*, 2546.
[15] A. Saneja, L. Sharma, R. D. Dubey, M. J. Mintoo, A. Singh, A. Kumar, P. L. Sangwan, S. A. Tasaduq, G. Singh, D. M. Mondhe, *Mater. Sci. Eng. Part C* **2017**, *73*, 616.
[16] L. Dai, D. Li, J. Cheng, J. Liu, L. H. Deng, L. Y. Wang, J. D. Lei, J. He, *Polym. Chem.* **2014**, *5*, 5775.
[17] P. Garcia-Oliveira, P. Otero, A. G. Pereira, F. Chamorro, M. Carpena, J. Echave, M. Fraga-Corral, J. Simal-Gandara, M. A. Prieto, *Pharmaceuticals* **2021**, *14*, 157.
[18] A. Saneja, R. Kumar, A. Singh, R. D. Dubey, M. J. Mintoo, G. Singh, D. M. Mondhe, A. K. Panda, P. N. Gupta, *Int. J. Pharm.* **2017**, *531*, 153.
[19] A. Saneja, R. Kumar, M. J. Mintoo, R. D. Dubey, P. L. Sangwan, D. M. Mondhe, A. K. Panda, P. N. Gupta, *Mater. Sci. Eng.* **2019**, *98*, 764.
[20] A. Saneja, D. Arora, R. Kumar, R. D. Dubey, A. K. Panda, P. N. Gupta, *Ann. New York Acad. Sci.* **2018**, *1421*, 5.
[21] J. Sanchis, F. Canal, R. Lucas, M. J. Vicent, *Nanomedicine* **2010**, *5*, 915.
[22] L. Dai, C. X. Li, K. F. Liu, H. J. Su, B. Q. Chen, G. F. Zhang, J. He, J. D. Lei, *RSC Adv.* **2015**, *5*, 15612.
[23] L. Dai, X. Cao, K. F. Liu, C. X. Li, G. F. Zhang, L. H. Deng, C. L. Si, J. He, J. D. Lei, *J. Mater. Chem., B* **2015**, *3*, 3754.
[24] J. M. Tan, G. Karthivashan, S. Abd Gani, S. Fakurazi, M. Z. Hussein, *J. Mater. Sci.: Mater. Med.* **2016**, *27*, 1.
[25] F. B. Mullauer, L. van Bloois, J. B. Daalhuisen, M. S. Ten Brink, G. Storm, J. P. Medema, R. M. Schiffelers, J. H. Kessler, *Anti-Cancer Drugs* **2011**, *22*, 223.
[26] D. L. Cooper, S. Harirforoosh, *PLoS One* **2014**, *9*, e87326.
[27] J. Yu, L. Sun, J. Zhou, L. Gao, L. Nan, S. Zhao, T. Peng, L. Han, J. Wang, W. Lu, *Bioconjugate Chem.* **2017**, *28*, 2823.
[28] B. Semete, L. Booysen, L. Kalombo, B. Ramalapa, R. Hayeshi, H. S. Swai, *Int. J. Pharm.* **2012**, *424*, 115.
[29] P. Kumar, A. K. Singh, V. Raj, A. Rai, A. K. Keshari, D. Kumar, B. Maity, A. Prakash, S. Maiti, S. Saha, *Int. J. Nanomed.* **2018**, *13*, 975.
[30] D. Dutta, B. Paul, B. Mukherjee, L. Mondal, S. Sen, C. Chowdhury, M. C. Debnath, *Sci. Rep.* **2019**, *9*, 11506.
[31] A. Saneja, R. Kumar, A. Singh, R. D. Dubey, M. J. Mintoo, G. Singh, D. M. Mondhe, A. K. Panda, P. N. Gupta, *Int. J. Pharm.* **2017**, *531*, 153.
[32] B. Shkodra-Pula, C. Grune, A. Traeger, A. Vollrath, S. Schubert, D. Fischer, U. S. Schubert, *Int. J. Pharm.* **2019**, *566*, 756.

[33] H. K. Makadia, S. J. Siegel, *Polymers* **2011**, *3*, 1377.
[34] S. Galindo-Rodriguez, E. Allemann, H. Fessi, E. Doelker, *Pharm. Res.* **2004**, *21*, 1428.
[35] U. Bilati, E. Allémann, E. Doelker, *Eur. J. Pharma. Sci.* **2005**, *24*, 67.
[36] S. Cîntă-Pînzaru, C. A. Dehelean, C. Soica, M. Culea, F. Borcan, *Chem. Cent. J.* **2012**, *6*, 1.
[37] E. E. Kovač-Bešović, K. Durić, Z. Kalo̵dera, E. Sofić, *Bosn. J. Basic Med. Sci.* **2009**, *9*, 31.
[38] J. M. Tan, G. Karthivashan, P. Arulselvan, S. Fakurazi, M. Z. Hussein, *Drug Des. Dev. Ther.* **2014**, *8*, 2333.
[39] Y. Zhang, R. Zhang, U. E. Illangakoon, A. H. Harker, C. Thrasivoulou, M. Parhizkar, M. Edirisinghe, C. J. Luo, *Int. J. Nanomed.* **2020**, *15*, 5389.
[40] S. B. Sun, P. Liu, F. M. Shao, Q. L. Miao, *Int. J. Clin. Exp. Med.* **2015**, *8*, 19670.
[41] C. Engineer, J. Parikh, A. Raval, *Trends Biomater. Artif. Organs* **2011**, *25*, 79.
[42] J. Panyam, D. Williams, A. Dash, D. Leslie-Pelecky, V. Labhasetwar, *J. Pharm. Sci.* **2004**, *93*, 1804.
[43] B. C. Hancock, M. Parks, *Pharma. Res.* **2000**, *17*, 397.
[44] S. Byrn, R. Pfeiffer, M. Ganey, C. Hoiberg, G. Poochikian, *Pharma. Res* **1995**, *12*, 945.
[45] S. Li, J. Zhang, Y. Fang, J. Yi, Z. Lu, Y. Chen, B. Guo, *Drug Des. Dev. Ther.* **2020**, *2020*, 243.
[46] R. Wang, X. Wang, X. Jia, H. Wang, W. Li, J. Li, *Int. J. Pharma.* **2020**, *588*, 119799.
[47] I. Amjadi, M. Rabiee, M. S. Hosseini, *Iran. J. Pharma. Res.* **2013**, *12*, 623.
[48] S. C. Endres, L. C. Ciacchi, L. Mädler, *J. Aerosol Sci.* **2021**, *153*, 105719.
[49] H. Vu-Quang, M. S. Vinding, D. Xia, T. Nielsen, M. G. Ullisch, M. Dong, N. C. Nielsen, J. Kjems, *Carbohydr. Polym.* **2016**, *136*, 936.
[50] N. Arunkumar, M. Deecaraman, C. Rani, *Asian J. Pharma.* **2009**, *3*, 168.
[51] A. R. do Vale Morais, É. N. Alencar, F. H. X. Júnior, C. M. De Oliveira, H. R. Marcelino, G. Barratt, H. Fessi, E. S. T. Do Egito, A. Elaissari, *Int. J. Pharm.* **2016**, *503*, 102.
[52] M. E. Fox, F. C. Szoka, J. M. Fréchet, *Acc. Chem. Res.* **2009**, *42*, 1141.
[53] H. Kobayashi, R. Watanabe, P. L. Choyke, *Theranostics* **2013**, *4*, 81.
[54] O. B. Flekhter, L. R. Nigmatullina, L. A. Baltina, L. T. Karachurina, F. Z. Galin, F. S. Zarudii, G. A. Tolstikov, E. I. Boreko, N. I. Pavlova, S. N. Nikolaeva, O. V. Savinova, *Pharma. Chem. J.* **2002**, *36*, 484.
[55] S. Jäger, K. Winkler, U. Pfüller, A. Scheffler, *Planta Med.* **2007**, *73*, 157.
[56] W. N. Ibrahim, L. Muizzuddin Bin Mohd Rosli, A. A. Doolaanea, *Int. J. Nanomed.* **2020**, *15*, 8059.
[57] R. Csuk, *Expert Opin. Ther. Pat.* **2014**, *24*, 913.
[58] A. Saneja, D. Nayak, M. Srinivas, A. Kumar, V. Khare, A. Katoch, A. Goswami, R. A. Vishwakarma, S. D. Sawant, P. N. Gupta, *Eur. J. Pharm. Sci.* **2017**, *97*, 79.
[59] J. Yoo, Y. Y. Won, *ACS Biomater. Sci. Eng.* **2020**, *6*, 6053.
[60] X. Huang, C. S. Brazel, *J. Control. Release* **2001**, *73*, 121.
[61] F. Alexis, *Polym. Inter.* **2005**, *54*, 36.
[62] P. Zhao, M. Guan, W. Tang, N. Walayat, Y. Ding, J. Liu, *Fitoterapia* **2023**, *166*, 105470.
[63] J. Van Meerloo, G. J. Kaspers, J. Cloos, *Cell Sensitivity Assays: The MTT Assay*, Springer Link, Portsmouth, UK **2011**, 237.
[64] M. Trif, P. E. Florian, A. J. Roseanu, *Biomed. Mater. Res A* **2015**, *103*, 3599.
[65] S. Xiong, S. George, *Arch. Toxicol.* **2013**, *87*, 1075.
[66] K. S. Mosiane, E. E. Nweke, M. Balogun, P. N. Fru, *Polymers* **2023**, *15*, 448.
[67] M. S. Cartiera, K. M. Johnson, V. Rajendran, M. J. Caplan, W. M. Saltzman, *Biomater* **2009**, *30*, 2790.
[68] D. Mundekkad, W. C. Cho, *Int. J. Mol. Sci.* **2022**, *23*, 1685.
[69] A. Saneja, R. Kumar, M. J. Mintoo, R. D. Dubey, P. L. Sangwan, D. M. Mondhe, A. K. Panda, P. N. Gupta, *Mater. Sci. Eng. Part C* **2019**, *98*, 764.
[70] V. Khare, A. Singh, G. Mahajan, N. Alam, S. Kour, M. Gupta, A. Kumar, G. Singh, S. K. Singh, A. K. Saxena, D. M. Mondhe, *Eur. J. Pharm. Sci.* **2016**, *92*, 183.
[71] N. Sharma, R. M. Kumari, N. Gupta, A. Syed, A. H. Bahkali, S. Nimesh, *Molecules* **2020**, *25*, 4243.
[72] M. Ferrari, M. C. Fornasiero, A. M. Isetta, *J. Immunol. Methods* **1990**, *131*, 165.

